

## Inhibition of *Stenotrophomonas maltophilia* dihydrofolate reductase by methotrexate: A single slow-binding process

M. D. NAVARRO-MARTÍNEZ<sup>1</sup>, J. CABEZAS-HERRERA<sup>2</sup>, F. GARCÍA-CÁNOVAS<sup>1</sup>, & J. N. RODRÍGUEZ-LÓPEZ<sup>1</sup>

<sup>1</sup>Grupo de Investigación de Enzimología, Departamento de Bioquímica y Biología Molecular A, Facultad de Biología, Universidad de Murcia, E-30100 Espinardo, Murcia, Spain, and <sup>2</sup>Servicio de Análisis Clínicos, Hospital, Universitario Virgen de la Arrixaca, Murcia, Spain

(Received 14 July 2006; in final form 30 October 2006)

### Abstract

Although antifolates such as trimethoprim are used in the clinical treatment of *Stenotrophomonas maltophilia* infection, the dihydrofolate reductase (DHFR) of this microorganism is scarcely known because it has never been isolated. Here, we describe the purification of this enzyme and kinetically characterize its inhibition by methotrexate (MTX). Upon MTX treatment, time-dependent, slow-binding inhibition was observed due to the generation of a long-lived, slowly dissociating enzyme-NADPH-inhibitor complex. Kinetic analysis revealed a one-step inhibition mechanism ( $K_I = 28.9 \pm 1.9$  pM) with an association rate constant ( $k_i$ ) of  $3.8 \times 10^7$  M<sup>-1</sup>s<sup>-1</sup>. Possible mechanisms for MTX binding to *S. maltophilia* DHFR are discussed.

**Keywords:** *Stenotrophomonas maltophilia*, dihydrofolate reductase, methotrexate, antifolates, slow-binding inhibitors

### Introduction

*Stenotrophomonas maltophilia* has emerged as an important nosocomial pathogen, especially in patients compromised by debilitating diseases, and is associated with increasing case/fatality ratios. The major risk factors associated with *S. maltophilia* infections include long-term hospitalization, previous antimicrobial therapy, fungal infections, catheterization and mechanical ventilation. *S. maltophilia* infection can cause bacteraemia, endocarditis, pneumonia, mastoiditis, peritonitis, meningitis, or infections of the eye, bone, joints, urinary tract, soft tissue and wounds [1,2]. The management of infections caused by *S. maltophilia* is particularly difficult because of the inherent resistance to many currently available broad-spectrum antimicrobial agents [3,4]. The treatment of choice for *S. maltophilia* infection is trimethoprim-sulfamethoxazole (TMP-SMZ; cotrimoxazole) alone or in

combination with ticarcillin-clavulanate [5]. TMP-SMZ is bacteriostatic for most isolates, hence high doses (12–15 mg/kg/day based on TMP) are usually recommended. Both drugs block the folic acid metabolism cycle of bacteria and are much more active together than either agent alone. Sulfonamides are competitive inhibitors of the incorporation of *p*-aminobenzoic acid, while TMP is an inhibitor of the dihydrofolate reductase (DHFR; 5,6,7,8-tetrahydrofolate: NADP<sup>+</sup> oxidoreductase, EC 1.5.1.3) reaction. It is well known that DHFR catalyzes the NADPH-dependent reduction of 7,8-dihydrofolate (DHF) to 5,6,7,8-tetrahydrofolate (THF), which acts as a coenzyme for a number of one-carbon transfer reactions including the reactions involved in nucleotide biosynthesis. Consequently, inhibition of DHFR leads to a disruption of DNA synthesis and this disruption is the basis of the antibiotic action of DHFR inhibitors, the

Correspondence: J. N. Rodríguez-López, Grupo de Investigación de Enzimología, Departamento de Bioquímica y Biología Molecular A, Facultad de Biología, Universidad de Murcia, E-30100 Espinardo, Murcia, Spain. E-mail: neptuno@um.es

antifolates [6]. Although TMP is currently used for the treatment of *S. maltophilia* infections, the mechanism by means of which this type of compound inhibits *S. maltophilia* DHFR has not been well characterized. Therefore, in this study we have purified the DHFR from this microorganism and present data of the inhibition of this enzyme by the classical antifolate compound, methotrexate (MTX).

## Materials and methods

### Enzyme isolation

A cotrimoxazole susceptible strain of *S. maltophilia* was collected at the University Hospital Virgen de la Arrixaca (Murcia, Spain). Bacteria were frozen at  $-70^{\circ}\text{C}$  in glycerol-meat medium. For the DHFR extraction, bacteria were inoculated onto MacConkey agar (Oxoid Ltd., Basingstoke, England) 24 h before use. Liquid medium, Brilliant Green Bile 2% broth (Oxoid), was then inoculated with the isolates and these broth cultures were incubated aerobically at  $37^{\circ}\text{C}$  and shaken at 100 cycles per min. Bacteria were grown to mid-log phase, harvested by centrifugation (1,600 rpm, 30 min) and washed twice in 50 mM phosphate buffer (pH 7.0) followed each time by a new centrifugation (1,600 rpm, 5 min). Cell lysis, centrifugation, and dialysis, were carried out between 4 and  $8^{\circ}\text{C}$ , while fast protein liquid chromatography (FPLC) purification steps were performed at room temperature. Cell paste from 2 L of culture (approximately 10 g of bacteria) was suspended in 30 mL of buffer A (5 mM Tris-HCl, pH 7.4, 1 mM EDTA) containing 0.1 mM phenylmethylsulfonyl fluoride as a protease inhibitor, and the cell suspension was homogenized in a Potter homogenizer followed by ultrasonication. After centrifugation at 36,000 rpm for 30 min to remove cell debris, the supernatant was filtered. This supernatant was brought to 40% saturation with solid ammonium sulfate under continuous stirring. After 1 h, the solution was centrifuged at 35,000 rpm for 30 min and the pellet was discarded. Additional ammonium sulfate was added to the clear supernatant to give 90% saturation and stirred for 1 h. After centrifugation, the precipitates were suspended in 2 mL of buffer B (10 mM potassium phosphate buffer, pH 7.4, 2 mM  $\beta$ -mercaptoethanol). Concentrated enzyme (2 mL samples) was loaded onto a gel-filtration column (Sephacryl S-75 26/60 Hi-Prep, Amersham Pharmacia Biotech Europe GmbH, Barcelona, Spain), equilibrated with buffer B and eluted at 0.5 mL/min. The active fractions were applied to an MTX-agarose (Sigma) column equilibrated with 50 mM potassium phosphate buffer, pH 6.5, containing 100 mM KCl. The column was then washed with 200 mL 50 mM potassium phosphate buffer, pH 6.5, containing 2 M KCl. The enzyme was eluted using 10 mL of 50 mM

Tris-HCl pH 8.6 containing 1 M KCl and 2 mM folic acid. Fractions containing DHFR activity were combined, dialyzed overnight against  $3 \times 2$  L buffer B, concentrated in an Amicon concentrator (YM-10 membrane) and stored at  $-80^{\circ}\text{C}$ . The DHFR concentration was determined by protein concentration determination using the Bio-Rad protein assay procedure with bovine serum albumin as standard. The homogeneity of enzyme samples were confirmed by the presence of a single band in SDS-PAGE gels with silver staining.

### DHFR assay

DHF was obtained from Aldrich Chemie GmbH (Madrid, Spain) and NADPH from Sigma. The activity of DHFR was determined at  $25^{\circ}\text{C}$  by following the decrease of NADPH and DHF in absorbance measurements at 340 nm ( $\epsilon = 11,800\text{M}^{-1}\text{cm}^{-1}$ ) using a Perkin-Elmer Lambda-2 spectrophotometer with cuvettes of 1.0 cm light-path. Temperature was controlled at  $25^{\circ}\text{C}$  using a Haake D1G circulating bath with a heater/cooler and checked using a Cole-Parmer digital thermometer with a precision of  $\pm 0.1^{\circ}\text{C}$ . Experiments were performed in a buffer containing 2-(*N*-morpholino)ethanesulfonic acid (Mes, 0.025 M), sodium acetate (0.025 M), tris(hydroxymethyl)aminomethane (Tris 0.05 M), and NaCl (0.1 M). The pH of the reaction was measured before and after the experiment. The assays were started by adding the enzyme. In the absence of the enzyme, the rate of change of absorbance was negligible. The concentrations of DHFR, NADPH, and DHF are given in the text or in the legends to the figures. The values of the maximum steady-state rate ( $V_{\text{max}}$ ) and the Michaelis constant of DHFR for DHF ( $K_m^{\text{DHF}}$ ) and NADPH ( $K_m^{\text{NADPH}}$ ) were determined from the curvature evident in the plots of NADPH and DHF disappearance versus time (10 determinations). For  $K_m^{\text{DHF}}$  or  $K_m^{\text{NADPH}}$  determinations the initial concentration of saturating NADPH (100  $\mu\text{M}$ ) or DHF (200  $\mu\text{M}$ ) was considered as constant during the overall consumption of 10  $\mu\text{M}$  DHF or 20  $\mu\text{M}$  NADPH by the enzyme, respectively. Data were fitted by nonlinear regression to the integrated form of the Michaelis equation [7], using Marquart's algorithm [8] implemented in the Sigma Plot 2.01 for Windows (Sigma Plot SPSS Inc. Chicago, Illinois).

### MTX inhibition

For MTX inhibition, the slow development of DHFR inhibition was determined by continuously monitoring the disappearance of NADPH and DHF after initiation of the reaction by the addition of DHFR. Reaction mixtures contained buffer, NADPH (100  $\mu\text{M}$ ), DHF (10  $\mu\text{M}$ ) and various concentrations of MTX. The extent of recovery of enzymatic activity

following inhibition induced by preincubation with DHFR inhibitors was determined as follows. DHFR was preincubated for 30 min at 25°C in the buffer mixture containing MTX. An aliquot of the incubation mixture was then diluted 500-fold into a reaction mixture containing buffer mixture, NADPH (100  $\mu\text{M}$ ) and DHF (10  $\mu\text{M}$ ). The recovery of enzyme activity was followed by continuous monitoring at 340 nm.

#### DHFR fluorescence studies

The fluorescence of DHFR is reduced upon substrate binding, and this property may be used as a convenient method for determining the dissociation constants of the enzyme-substrate complex. The dissociation constant for the binding of NADPH ( $K_d^A$ ) was determined by fluorescence titration in an automatic scanning Perkin-Elmer LS50B spectrofluorimeter with 1.0 cm light path cells, equipped with a 150 W xenon (XBO) light source. The formation of the binary complex between the enzyme and NADPH was followed by measuring the quenching of tryptophan fluorescence of the enzyme upon addition of microliter volumes of a concentrated stock solution of NADPH. Fluorescence emission spectra were recorded when DHFR fluorescence was excited at 290 nm. All measurements were corrected for dilution and the data from the titration curves were fitted as described previously [9]. Titrations were performed in the same buffers as described for DHFR assays. Temperature was controlled at 25°C using a Haake D1G circulating bath with a heater/cooler.

#### Kinetic simulations

Kinetic simulation experiments were carried out to confirm the mechanism proposed in Table II. The kinetics of this mechanism is defined by a set of differential equations, whose numerical integration was performed with a computer program designed by García-Sevilla et al. [10]. Experimentally determined values of the equilibrium and rate constants were assigned to the partial reactions defined in this scheme.

### Results and discussion

The  $K_m$  values for both substrates, NADPH and DHF, were determined using the purified enzyme. Due to the very  $K_m$  low values, we used the integrated Michaelis equation for their calculation (see Materials and Methods section). A graphical representation for the calculation of the  $K_m$  for DHF is presented in Figure 1. The  $K_m$  for NADPH was calculated to be  $12 \pm 3 \mu\text{M}$ , while that for DHF was  $1.8 \pm 0.4 \mu\text{M}$  at pH 7.4. These values are similar to the  $K_m$  values of DHFRs from other species [11]. From the calculated

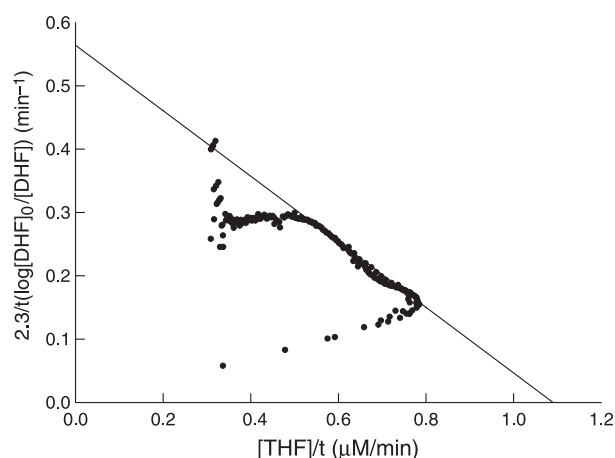


Figure 1. Plot of the integrated form of the Michaelis equation to a progress curve containing *S. maltophilia* DHFR (22 pM), NADPH (100  $\mu\text{M}$ ) and DHF (10  $\mu\text{M}$ ) at pH 7.4.

$V_{\max}$  value a catalytic constant of  $123 \pm 10 \text{ s}^{-1}$  was determined. When DHFR activity was continuously assayed after the addition of enzyme to assay mixtures containing MTX, DHF and NADPH, the resulting progress curves displayed a time-dependent decrease in the reaction rate before reaching a steady state velocity which varied as a function of inhibitor concentration (Figure 2A), suggesting the slow establishment of an equilibrium between enzyme, inhibitor and the enzyme-inhibitor complex. Thus, MTX acts as a slow-binding inhibitor. Further evidence for slow-binding inhibition was obtained by adding aliquots of preincubated mixtures of DHFR and MTX to substrates-containing assay mixtures. The resulting progress curves displayed a time-dependent increase in the reaction rate and reached a steady-state velocity identical to the velocity obtained without preincubation.

There are three simple mechanisms which can account for the slow onset of inhibition (Table I) [12]. The first (mechanism A) corresponds to an initial slow-binding process. In the second mechanism (mechanism B), an EI complex is formed rapidly and then undergoes slow isomerization (conformational change) to a slowly dissociating EI\* complex. In a third variant (mechanism C) the enzyme itself must slowly isomerize before it can bind the inhibitor. The kinetic analysis of the reaction progress curves recorded at pH 7.4 for MTX concentrations of up to 2 nM revealed that the initial reaction velocities ( $v_0$ ) were essentially concentration independent at lower inhibitor concentrations, whereas the velocities decreased at higher concentrations of MTX (Figure 2B). Furthermore, a replot of  $k_{\text{obs}}$  against the inhibitor concentrations (Figure 2C) gave a straight line with no indication of saturation kinetics. Both features are characteristic of mechanism A and indicate the direct formation of a slowly

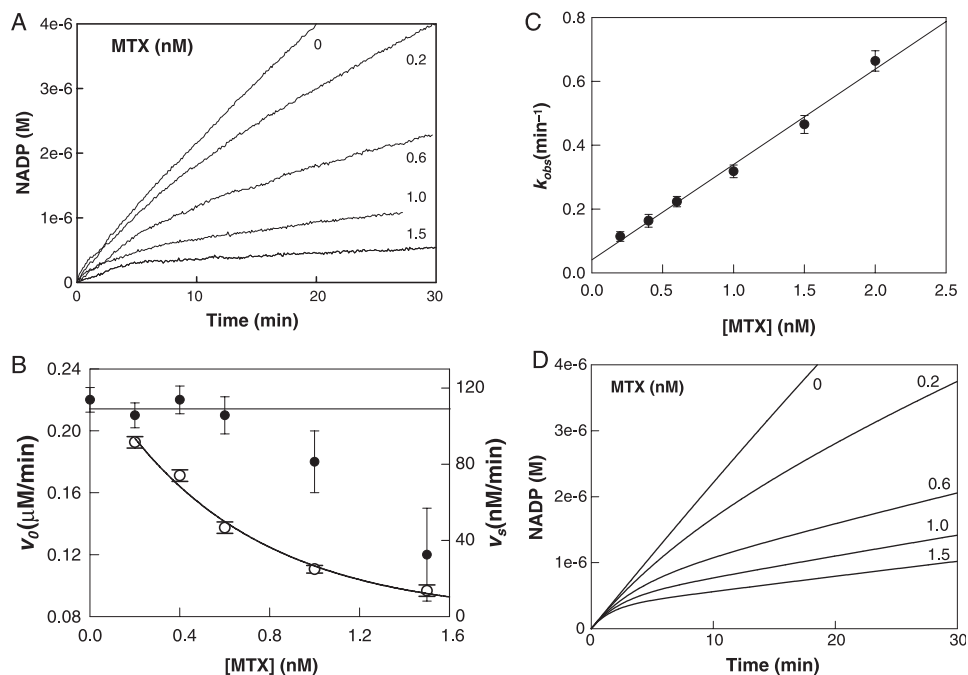


Figure 2. Inhibition of *S. maltophilia* DHFR activity by MTX at pH 7.4. (A) Experimental reaction progress curves at inhibitor concentrations of 0, 0.2, 0.6, 1.0, and 1.5 nM. The experimental conditions were: DHFR 40 pM; NADPH 100  $\mu$ M and DHF 10  $\mu$ M. (B) Replot of  $k_{obs}$  versus MTX concentration.  $k_{obs}$  values are derived from the progress curves as described in Equation (1). (C) Dependences of  $v_0$  (filled circles) and  $v_s$  (open circles) on MTX concentration. Solid lines represent the dependence of both parameters in simulation experiments. (D) Simulated reaction progress curves at inhibitor concentrations of 0, 0.2, 0.6, 1.0, and 1.5 nM. Concentration of enzyme and substrates were as for experimental results and the rate constants used for simulation of the mechanism of Table II were as described in Table III with  $k_4 = 10s^{-1}$ .

dissociating EI complex without the initial formation of a rapidly reversible enzyme-inhibitor complex.

Although the DHFR-catalysed reaction has been shown to occur via a random mechanism [13,14], it can be simplified to an ordered mechanism whenever  $[NADPH] \gg [DHF]$ . Although it is known that MTX, a competitive inhibitor, can interact with both the free enzyme and the E-NADPH complex, under the above experimental conditions the most plausible mechanism is depicted in Table II. Provided

that the concentration of free inhibitor is not substantially altered by the formation of an enzyme-NADPH-inhibitor complex, the progress curve for the inhibition in the presence of saturating NADPH can be described by Equation (1):

$$P = v_s t + (v_0 - v_s)(1 - \exp(-k_{obs}t))/k_{obs} \quad (1)$$

where  $v_s$ ,  $v_0$  and  $k_{obs}$  represent the steady-state velocity, initial velocity and apparent first-order rate constant, respectively. A complete kinetic analysis of the mechanism described in Table II rendered complex expressions for  $k_{obs}$ ,  $v_0$  and  $v_s$  (Table II) as a function of the concentrations of substrates, NADPH (A) and DHF (B), and the inhibitor MTX (I). The apparent first-order rate constant is related to the inhibitor concentration by Equation (2) where  $k_i^{app}$  denotes the apparent association second-order rate constant for the binding of MTX to the enzyme-NADPH complex:

$$k_{obs} = k_i^{app}[I] + k_{-i} \quad (2)$$

$$k_i^{app} = k_i \alpha \quad (3)$$

$$\alpha = K_m^B[A]/(K_d^A K_m^B + K_m^B[A] + K_m^A[B] + [A][B]) \quad (4)$$

A plot of  $k_{obs}$  versus  $[I]$  gave a straight line which intercepts the ordinate axis at  $k_{-i}$  ( $1.1 \times 10^{-3} s^{-1}$ ).

Table I. Different mechanisms to explain slow-binding inhibition of *S. maltophilia* by MTX.

Mechanism	Model
A	$E \xrightleftharpoons[k_{-i}]{k_i[I] \text{ (slow)}} EI$
B	$E \xrightleftharpoons[k_{-i}]{k_i[I]} EI \xrightleftharpoons[k_{-t}]{k_t \text{ (slow)}} EI^*$
C	$E \xrightleftharpoons[k_{-i}]{k_i \text{ (slow)}} E^* \xrightleftharpoons[k_{-t}]{k_t[I]} E^*I$

Table II. Possible mechanisms for the slow-binding inhibition of *S. maltophilia* DHFR assuming an initial slow-binding process and their relationship to the apparent first-order rate constant ( $k_{obs}$ ) and steady-state rates  $v_0$  and  $v_s$ . (E = DHFR, A = NADPH, B = DHF and I = MTX).

Mechanism	$k_{obs}$	Steady-state rates
$  \begin{array}{c}  E + A \xrightleftharpoons[k_2]{k_1} E-A + B \xrightleftharpoons[k_4]{k_3} E-A-B \xrightarrow{k_5} E + P + Q \\  + I \xrightleftharpoons[k_{-i}]{k_i} E-A-I \quad \text{(slow)}  \end{array}  $	$k_{obs} = k_i \alpha [I] + k_{-i}$ $\alpha = K_m^B [A] / (K_d^A K_m^B + K_m^B [A] + K_m^A [B] + [A][B])$	$v_0 = \frac{V_{max} [A][B]}{K_d^A K_m^B + K_m^B [A] + K_m^A [B] + [A][B]}$ $v_s = \frac{V_{max} [A][B]}{K_d^A K_m^B + K_m^B \left( 1 + \frac{[I]}{K_i} \right) [A] + K_m^A [B] + [A][B]}$

where  $K_d^A = k_2/k_1$ ,  $K_m^A = k_5/k_1$ ,  $k_m^B = (k_4 + k_5)/k_3$ , and  $K_i^{EA} = k_{-i}/k_i$

From the slope of this line a  $k_i^{app}$  of  $5.3 \times 10^6 \text{ M}^{-1}\text{s}^{-1}$  could be determined and an apparent inhibition constant ( $k_i^{app} = k_{-i}/k_i^{app}$ ) of 0.21 nM was calculated.

The binding of NADPH to free *S. maltophilia* DHFR was assessed by following the decrease in enzyme fluorescence that occurs upon formation of the enzyme-NADPH complex. The data showed that the dissociation constant of free DHFR for NADPH ( $K_d^A$ ) was 5.2  $\mu\text{M}$ , which was similar to the value found for the binding of NADPH to bovine DHFR (4.8  $\mu\text{M}$ ) [15]. By introducing the concentration of the substrates and the calculated values for  $K_d^A$ ,  $K_m^A$  and  $K_m^B$  in Equation (4), the factor  $\alpha$  was calculated ( $\alpha = 0.14$ ), and the absolute value for the second-order constant for the binding of MTX to the E-NADPH complex ( $k_i$ ) had a value of  $3.8 \times 10^7 \text{ M}^{-1}\text{s}^{-1}$ . Thus, the absolute inhibition constant for the binding of MTX ( $K_i$ ) was 28.9 pM.

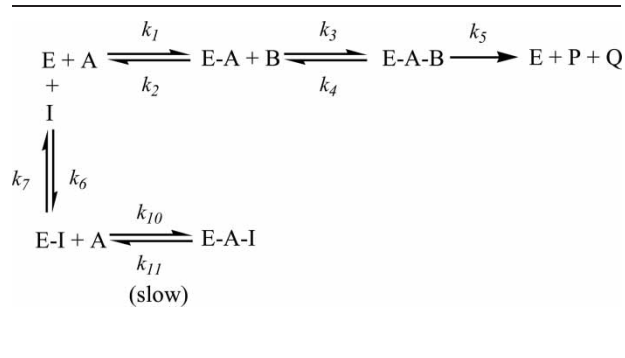
By using the expressions obtained in the kinetic analysis of the mechanism of Table II, and assuming steady-state conditions in the binding of DHF to the E-NADPH complex ( $k_4 \ll k_5$ ), the elemental rate constants were calculated (Table III). We used these constants for the numerical simulation of the mechanism. The simulated results are shown in Figures 2B and 2D, and are completely in accordance with the experimental recordings, demonstrating that the lower values of  $v_0$  determined at high MTX concentrations (Figure 2B) may be due to the lack of spectrophotometrical information concerning this parameter at short time periods.

DHFR has been isolated and characterized from a wide variety of bacterial and animal sources [11]. These enzymes differ with respect to their type of inhibition by MTX and other folate analogues [14]. Thus, although both MTX and TMP can be considered as slow tight-binding inhibitors of the enzyme from *E. coli*, only MTX gives this type of inhibition with the chicken liver enzyme. Although the exact structural basis that determines the type of inhibition is not well known, it might be related with the interaction of the drugs with particular residues of

Table III. Kinetic constants for the reaction of *S. maltophilia* DHFR with NADPH and DHF at 25°C, pH 7.4, and its inhibition by MTX.

Constant	Value
$K_d^A$ ( $\mu\text{M}$ )	5.2
$K_m^A$ ( $\mu\text{M}$ )	12
$K_m^B$ ( $\mu\text{M}$ )	1.8
$K_i$ (pM)	28.9
$k_5$ or $k_{cut}$ ( $\text{s}^{-1}$ )	123
$k_1$ ( $\text{M}^{-1}\text{s}^{-1}$ )	$1.3 \times 10^7$
$k_2$ ( $\text{s}^{-1}$ )	68
$k_3$ ( $\text{M}^{-1}\text{s}^{-1}$ )	$6.3 \times 10^7$
$k_i$ ( $\text{M}^{-1}\text{s}^{-1}$ )	$3.8 \times 10^7$
$k_{-i}$ ( $\text{s}^{-1}$ )	$1.1 \times 10^{-3}$

Table IV. Possible mechanism for the slow-binding inhibition of DHFR (E) assuming the formation of a slow dissociating complex after the reaction of NADPH (A) with the enzyme-inhibitor complex. B represents DHF and I is MTX.



the DHFR active site. The results obtained here show that MTX is an effective inhibitor of *S. maltophilia* DHFR, and that the origin of the slow inhibition is due to a single initial slow-binding process. This mechanism differs from the mechanism proposed for the inhibition of several DHFRs by MTX, which was mechanism B of Table I [14]. Recently the origin of the slow-binding inhibition of bovine liver DHFR with epigallocatechin-3-gallate (EGCG) and other antifolates has been discussed [15]. It was confirmed that EGCG is a competitive inhibitor with respect to DHF, which preferentially binds to the free enzyme. The origin of its slow-binding inhibition is the formation of a slow dissociation ternary complex by the reaction of NADPH with the E-I complex. A more complete scheme of this mechanism is observed in Table IV. An identical mechanism could explain the slow binding inhibition observed with MTX for several enzyme sources [14]. It is known that MTX can bind efficiently to the free enzyme [16] and that NADPH can form a ternary complex by binding to the E-MTX complex [17]. The kinetic data presented here clearly show that in *S. maltophilia* the formation of the ternary complex is precluded; however, further experiments to determine the sequence and structure of this new isolate DHFR are needed to better understand the basis of its interactions with MTX. Although the crystal structure of many DHFRs, including the human enzyme, have been solved in recent years, the exact structural basis that determines the binding of MTX to *S. maltophilia* DHFR cannot be exactly deduced until the crystal structure for this enzyme is determined. Great differences in the structural basis of binding of other antifolate drugs to eukaryotic and prokaryotic DHFR have been observed and are the starting point for the development of new antibiotics without side-effects on humans. Although MTX is very active against *S. maltophilia*, its clinical use is precluded since it is also a strong inhibitor of human

DHFR, and therefore, may present many adverse side-effects. The data presented here could be of interest to explain the DHFR inhibition mechanisms of MTX and other natural or synthetic antifolates. To our knowledge the mechanism of *S. maltophilia* DHFR inhibition by MTX is unique and we hereby describe a complete kinetic analysis for the calculation of its inhibition kinetic constants that could be of help in the search for new DHFR inhibitors.

### Acknowledgements

This work was supported in part by a grant from PBL International to J.N.R-L and from Fondo de Investigaciones Sanitarias (FIS) (Project 01/3025) and Red Temática de Investigación Cooperativa de Centros del Cáncer (RTICCC) (Red de centros C03/10) to J.C-H. M.D.N-M has a fellowship from Fundación Séneca, Murcia, Spain. We thank Dr. Joaquín Ruiz-Gómez at the Servicio de Microbiología del Hospital Clínico Universitario Virgen de la Arrixaca for providing us with the *S. maltophilia* clinical isolates.

### References

- [1] Irifune K, Ishida T, Shimoguchi K, Ohtake J, Tanaka T, Morikawa N, Kaku M, Koga H, Kohno S, Hara K. *J Clin Microbiol* 1994;32:2856.
- [2] Klausner JD, Zukerman C, Limaye AP, Corey L. *Infect Control Hosp Epidemiol* 1999;20:756.
- [3] Denton M, Kerr KG. *Clin Microbiol Rev* 1998;11:57.
- [4] Elting LS, Khardori N, Bodey GP, Fainstein V. *Infect Control Hosp Epidemiol* 1990;11:134.
- [5] Poulos CD, Matsumura SO, Willey BM, Low DE, McGeer A. *Antimicrob Agents Chemother* 1995;39:2220.
- [6] Gready JE. *Adv Pharmacol Chemother* 1980;17:37.
- [7] Cornish-Bowden A. *In: Fundamentals of Enzyme Kinetics*. London: Butterworth and Co; 1979. p 34–37.
- [8] Marquardt DW. *J Soc Ind Appl Math* 1963;11:431.
- [9] Williams JW, Morrison JF, Duggleby RG. *Biochemistry* 1979;18:2567.
- [10] García-Sevilla F, Garrido del Solo C, Duggleby RG, García-Cánovas F, Peyro-García R, Varón R. *BioSystems* 2000;54:151.
- [11] Wilquet V, Gaspar JA, van de Lande M, Van de Castele M, Legrain C, Meiering EM, Glansdorff N. *Eur J Biochem* 1998;255:628.
- [12] Clausen T, Huber R, Messerschmidt A, Pohlentz HD, Laber B. *Biochemistry* 1997;36:12633.
- [13] Rod TH, Radkiewicz JL, Brooks CL III. *Proc Natl Acad Sci USA* 2003;100:6980.
- [14] Stone SR, Morrison JF. *Biochim Biophys Acta* 1986;869:275.
- [15] Navarro-Perán E, Cabezas-Herrera J, Hiner ANP, Sadunishvili T, García-Canovas F, Rodríguez-López JN. *Biochemistry* 2005;44:7512.
- [16] Williams JW, Morrison JF, Duggleby RG. *Biochemistry* 1979;18:2567.
- [17] Dunn SMJ, King RW. *Biochemistry* 1980;19:766.